Different scenarios for the in-plane spin reorientation transition in Fe(110) films on W(110)

T. Ślęzak,[1,*] M. Zając,[1,2,†] M. Ślęzak,[1] K. Matlak,[1] A. Kozioł-Rachwał,[1] D. Wilgocka-Ślęzak,[3] A. I. Chumakov,[2] R. Rüffer,[2] and J. Korecki[1,3]

[1]*Faculty of Physics and Applied Computer Science, AGH University of Science and Technology, 30-059 Kraków, Poland*

[2]*European Synchrotron Radiation Facility, Boîte Postale 220, F-38043 Grenoble Cedex, France*

[3]*Jerzy Haber Institute of Catalysis and Surface Chemistry, Polish Academy of Sciences, 30-239 Kraków, Poland*

(Received 13 December 2012; published 26 March 2013)

We investigated the spin reorientation transition during the growth of Fe(110) films on W(110) at 250 °C using the *in situ* nuclear resonant scattering of x rays. The measurements as a function of the grazing incidence angle demonstrated that the spin reorientation proceeds via an intermediate, noncollinear magnetic state, and with increasing thickness, the magnetization reorientation from the $[1\bar{1}0]$ to the [001] direction is activated at the film surface and completed at the Fe/W interface. Furthermore, as the temperature was decreased from 250 °C to 160 °C, the temperature-driven spin reorientation transition (SRT) between the [001] and $[1\bar{1}0]$ directions was observed with a similar noncollinear transient magnetic state. The thickness-temperature SRT phase diagram was schematically drawn.

DOI: 10.1103/PhysRevB.87.094423 PACS number(s): 75.75.−c, 76.80.+y, 75.70.Ak

I. INTRODUCTION

Over the past decades, controlling the spin direction in magnetic nanostructures has become one of the key tasks in nanomagnetism because it is mandatory for magnetic recording technological applications. From this point of view, the spin reorientation transition (SRT), which consists of switching the spontaneous magnetization orientation between two directions in space, plays an important role.[1] The SRT provides an opportunity to obtain a desired magnetization direction by adjusting the film thickness,[2] temperature,[3] or coating material[4] because in this way, the competition between various magnetic anisotropies, such as the shape, magnetocrystalline, magnetoelastic, or surface anisotropy, can be adjusted. The importance and effectiveness of the SRT in controlling the magnetization direction has been demonstrated in numerous experiments, primarily in the case of polar SRT processes in which the spin orientation switches between the out-of-plane and an in-plane direction as the film thickness increases or the temperature changes.[2,3] One of the fundamental problems for characterizing the SRT process is determining the route in which this transition proceeds. Knowledge about the magnetization reorientation process not only provides deeper insight into the physics of the SRT by indicating its discontinuous (first-order) or continuous (second-order) character but also, in many cases, highlights the role of specific magnetic anisotropy contributions.[5] The three classes of the SRT scenarios have been theoretically predicted[5] and experimentally confirmed, including the formation of magnetic domains,[6] coherent magnetization rotation,[7,8] and the formation of a vertical or lateral noncollinear magnetic structure.[9] While the first two mentioned possibilities assume a homogenous magnetization along the film normal, the third one allows for finite differences between the magnetization directions of the neighboring atomic sublayers that may lead to the formation of a planar Bloch-like domain wall. In our recent work, we have demonstrated such a complex behavior during the thickness-induced SRT for the Fe(110)/W(110) system.[9] In this system, the magnetization direction switches from the $[1\bar{1}0]$ to the [001] in-plane direction during the film growth process as the thickness of the iron film approaches a critical thickness, d_c. While earlier explanations of this SRT process, including the one that assumes the key role of magnetic surface anisotropy[4,10] and the other based on the evolution of the magnetoelastic anisotropy,[11] implicitly ruled out any vertical magnetic noncollinearities during the magnetization reorientation, the nature of the transition appeared to be more complex.[9]

We demonstrated that the room temperature (RT) in-plane SRT from the $[1\bar{1}0]$ to the [001] direction is initiated at the deepest layers (neighboring to the tungsten substrate). With increasing thickness, the magnetization of the subsequent sublayers rotates and the transition is finally completed at the surface layers. This result indicates that a strong surface anisotropy pins the magnetization to the $[1\bar{1}0]$ direction, whereas the SRT itself can be attributed to the changes of the strain-induced magnetoelastic anisotropy that evolve with the thickness during the growth of the film. Therefore, at the vicinity of the critical thickness, a vertical noncollinear magnetic state exists with a large spread of the magnetization orientation at the film surface and at the Fe/W interface. This behavior cannot be treated within the common phenomenological description of the SRT that is based on the separation of the total magnetic anisotropy into the surface and volume contributions, which works for the homogenous magnetization approximation, but exceptionally, the role of particular magnetic anisotropy contributions in the magnetic reorientation could be identified.

It is especially convincing that the details of the transition predominantly depend on the stress-strain structure assisted by a contribution of the magnetic surface anisotropy. This dependence implies an immediate question concerning the scenario of the other possible SRT processes for Fe/W(110), such as a thickness-induced transition at elevated temperatures and a temperature-induced transition, at which the structure of the film can evolve due to the thermal relaxation of the film that accompanies the transition. This paper reports on our investigations of these two issues with the use of *in situ* nuclear resonant scattering (NRS) of synchrotron

radiation. Compared to our previous NRS investigation of the thickness-induced SRT at RT,[9] we have explored an enhancement of the NRS depth sensitivity by varying the grazing incidence angle.[12,13] We have demonstrated that the thickness-induced SRT process at 250 °C also proceeds through an intermediate, vertical noncollinear magnetic state, but in contrast to the RT thickness-driven reorientation, the sequence of sublayer magnetization switching is opposite, namely, with the increasing thickness, the magnetization reorientation from the $[1\bar{1}0]$ to [001] direction is initiated at the surface atomic layers and completed at the Fe/W(110) interface. The temperature-induced SRT could be observed as the sample temperature was decreased after completion of the thickness-driven SRT at 250 °C. In this case, the scenario of the magnetization switching from the [001] magnetized state at 250 °C to the $[1\bar{1}0]$ magnetization orientation at 160 °C is similar to the thickness-driven SRT; the intermediate magnetic structure at 215 °C is strongly noncollinear with the topmost layers magnetized along the [001] direction and the bottom ones reoriented to the $[1\bar{1}0]$ direction. In addition, upon the subsequent temperature increase to 250 °C, the irreversibility of the SRT transition could be observed, which was most likely due to residual gas adsorption.

II. EXPERIMENTAL DETAILS: NRS TECHNIQUE AND SAMPLE PREPARATION

NRS is a synchrotron analog of Mössbauer spectroscopy in the sense that it involves a recoilless excitation (induced by the resonant x rays with an energy of 14.4 keV for ^{57}Fe) of the nuclear energy levels, which are split due to the hyperfine interactions.[14] The NRS method is based on the analysis of the characteristic beat pattern observed in the time evolution of the intensity of the nuclear resonant scattering (the so-called time spectrum), and it yields the site and layer selective determination of hyperfine magnetic fields and electric field gradients with precise information about their orientation. Moreover, NRS can also distinguish between ferromagnetic, antiferromagnetic, or noncollinear ordering in the sample, thus allowing the determination of a sublattice and, in the case of layered systems, sublayer magnetic order.[15] It is also important that virgin magnetic states are accessible because no magnetic field is required to probe the local magnetization vector by the hyperfine interactions.

For surfaces and thin films, the NRS technique is performed in the grazing incidence (GI) geometry. In this geometry, the intrinsic NRS depth sensitivity arises from the evanescent penetration depth of the x-ray radiation field for the incidence angles close to the Fe critical angle, and it strongly depends on the value of the grazing angle.[10] This process is illustrated in Fig. 1 via the simulated time spectra with the typical scattering geometry using purely σ-polarized incident radiation and unpolarized detection[16] for a 6-nm-thick Fe film on a tungsten substrate that are calculated for three GI angles: $\theta = 0.1^\circ$, 0.25°, and 0.35°. The simulations were performed using the CONUSS software package, which is based on the dynamical theory of nuclear resonant scattering[17] assuming a single value of a bulklike hyperfine magnetic field of $B_{\rm hf} = 33$ T in the film. In Fig. 1, the rows (a) and (c) correspond to the homogenously magnetized ^{57}Fe films with the magnetization oriented nearly parallel and perpendicular to the wave vector $\vec{k}_0$ of the incident x rays, respectively. Row (b) illustrates the case of a vertically inhomogeneous magnetization structure, which is composed of two 3-nm-thick Fe slabs with the orthogonal magnetization directions such that the magnetization of the upper part of the ^{57}Fe film is nearly parallel to $\vec{k}_0$. It can be clearly seen that the basic quantum beat features of the time spectra only slightly change with the grazing angle value for the homogenous magnetization, and they typically display a single frequency beat pattern for x rays that are parallel to the magnetization [row (a)] or a pattern that exhibits two frequencies and their linear combinations [row (c)], both corresponding to the common hyperfine magnetic splitting at $B_{\rm hf} = 33$ T but different orientation of the magnetic hyperfine field with respect to $\vec{k}_0$.[7] However, when the noncollinear magnetizations of the top and bottom parts of the Fe film are assumed [Fig. 1(b)], the time spectra are very sensitive to the grazing angle. The time spectrum for $\theta = 0.1^\circ$ is very similar to that for a homogenously magnetized film with the magnetization parallel to $\vec{k}_0$. The NRS is clearly predominantly sensitive to the top part of the Fe film for such low grazing angle values. The opposite situation is observed for grazing angles as high as $\theta = 0.35^\circ$. In this case, the spectrum of the noncollinear structure is almost indistinguishable from the one for the film magnetized perpendicular to the incident beam. This result indicates that NRS probes the bottom part of the Fe film for higher grazing angles, and it is almost completely insensitive to the topmost atomic layers. The above simulations well justify such a NRS measurement scheme in that the time spectra acquired for various grazing angles are used when the vertically noncollinear magnetic structure should be resolved.

The measurements were performed at the Nuclear Resonance Beamline (ID18) (Ref. 18) of the European Synchrotron Radiation Facility (ESRF) in Grenoble using a multichamber

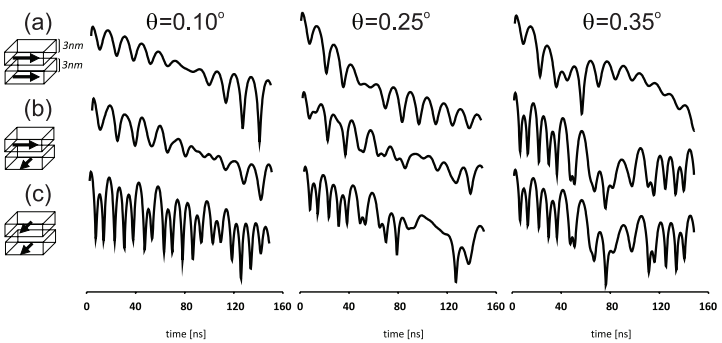

FIG. 1. The NRS time spectra for the 6-nm-thick Fe film on a tungsten substrate simulated for the three grazing incidence angles θ, assuming (a) homogenous in-plane magnetization parallel to the k vector of the x-ray beam, (b) in-plane noncollinear structure composed of the top 3-nm-thick sublayer with the magnetization parallel to the k vector of the x-ray beam and the bottom 3-nm-thick sublayer with an orthogonal magnetization orientation, and (c) homogenous in-plane magnetization perpendicular to the k vector of the x-ray beam. The intensity axis (not shown) is displayed in a logarithmic scale.

ultrahigh vacuum (UHV) system[19] that is equipped with standard surface preparation and characterization methods, such as molecular beam epitaxy, low-energy electron diffraction (LEED), and Auger electron spectroscopy. For this particular experiment, ^{57}Fe was deposited in the NRS chamber onto a freshly cleaned W(110) single crystal, which was prealigned to the x-ray beam with $\vec{k}_0$parallel to [001]. First, a 6-nm-thick epitaxial Fe(110) film was grown at RT. Because the NRS spectra were acquired during the film growth process, which enabled the running control of the film magnetic state, the deposition could be precisely stopped at a thickness that was slightly above the critical value of the thickness-driven SRT process,[9] when the magnetization switching from $[1\bar{1}0]$ to [001] was completed. The morphology of the Fe film deposited at RT is characterized by a rooflike surface modulation, as could be clearly seen in the scanning tunneling microscopy image (not shown) collected for a 5-nm-thick Fe film in a complementary UHV system, indicating that on the top of the continuous 4-nm-Fe-base layer, 1.2-nm-high islands, elongated along the $[1\bar{1}0]$ direction, with triangular cross sections, are formed, in agreement with previous LEED data.[20] For such a film, the magnetization reorientation transition back to $[1\bar{1}0]$ could be induced by increasing the temperature to 250 °C. The process responsible for this reentrant $[1\bar{1}0]$ magnetization easy direction was a surface smoothing, which was easily observed by sharpening of the LEED spots, that increases the critical value of the thickness-driven SRT process.[20] Therefore, the magnetic state with the $[1\bar{1}0]$ in-plane easy magnetization direction was stabilized at 250 °C. After 15 min of initial annealing at 250 °C, a slow add evaporation of ^{57}Fe has been started at this temperature with the rate 0.04 monolayer (ML) per minute (1 ML was taken as the equivalent of 0.2 nm). The character of the NRS time spectrum, which was already apparent after a few seconds of data acquisition, was continuously inspected during the deposition of Fe for the grazing incidence angle of $\theta = 0.25^\circ$ because for this intermediate θ value, the sensitivity of the NRS measurements to the magnetization structure of the entire Fe film is ensured. Furthermore, for certain deposition stages, the deposition was stopped for ∼2 min and NRS time spectra were collected at the constant thickness for three GI angles, $\theta = 0.1^\circ$, 0.25°, and 0.35°.

III. RESULTS AND DISCUSSION

Selected experimental time spectra, which were accumulated during the deposition of ^{57}Fe for the GI angle $\theta = 0.25^\circ$ using the scattering geometry as shown in Fig. 2(a) with $\vec{k}_0$ parallel to the [001] direction, are shown in Fig. 2(b) as a function of the increasing film thickness. The initial time spectrum measured for the thickness of $D = 6.0$ nm at 250 °C reveals a dense quantum beat structure that is characteristic for the orthogonal alignment of $\vec{k}_0$and the magnetization $\vec{M}$. Such a spectrum could be well fitted using the CONUSS software assuming a homogenous hyperfine magnetic field along $[1\bar{1}0]$ with $B_{\rm hf} = 31.0$ T, which is slightly less than the RT bulk-Fe value due to the temperature reduction of the magnetization. Within the experimental accuracy of ±0.1 T, this value remained unchanged for all other discussed spectra. Such a picture of a nearly uniform $B_{\rm hf}$ value across the film is consistent with the NRS (Ref. 21) and conversion electron Mössbauer spectroscopy data,[22,23] which indicates that the hyperfine interactions are only slightly modified in one surface and one interface iron monolayer compared to bulk Fe. As the deposition progressed, the spectra changed due to the thickness-induced SRT and, according to the theoretical fits, the state of uniform magnetization parallel to the [001] direction is achieved starting from the film thickness of $D = 6.9$ nm. Note that although no external magnetic field was applied during the growth of Fe, a small in-plane residual magnetic field, with components of ∼1 Oe along the $[1\bar{1}0]$ and [001] directions, was measured at the sample position. This field may easily erase the domains of the virgin state, especially because during the growth process, the Fe film undergoes a thickness-induced paramagnetic-ferromagnetic phase transition at which the magnetic susceptibility becomes infinite.

The transition is not instantaneous, which is in contrast to the results Vescovo *et al.* obtained for Fe(110) microwedges.[24] The onset of the SRT process was identified for the Fe thickness of $D = 6.2$ nm, which was when the first changes in the shape of the time spectra could be observed. Then, the SRT process gradually develops along with the Fe deposition via an intermediate state that is well represented by the spectrum for the thickness of $D = 6.6$ nm, which substantially differs from the time spectra of the two homogenous magnetization states discussed above. As shown by Röhlsberger *et al.*,[16] in such a case, a single time spectrum might not be sufficient to unambiguously determine the spin structure. Therefore, the analysis of the complex spin configuration during the magnetization reorientation was based on the NRS measurements performed as a function of the GI angle, as exemplified for $D = 6.6$ nm in Fig. 2(c). The time spectra measured for $\theta = 0.1^\circ$, 0.25°, and 0.35° are characterized by a strong variation of the bit structure as a function of the grazing incidence angle. The spectrum for $\theta = 0.1^\circ$ has a simple beat structure, which indicates that the magnetization of the top part of the Fe film with a thickness of ∼3 nm is aligned with $\vec{k}_0$, i.e., it has reoriented to the [001] direction. However, the time spectrum collected for $\theta = 0.35^\circ$ has a dense beat structure that is typical for the magnetization perpendicular to $\vec{k}_0$, which means that the magnetization direction of the Fe slab that neighbors the tungsten substrate is still parallel to the $[1\bar{1}0]$ direction. The described differences in the shapes of the experimental time spectra for low and high grazing angles at this intermediate thickness are consistent with the simulated time spectra of the 6-nm-thick Fe film composed of two equivalent slabs with orthogonal magnetizations (Fig. 1) and provide direct evidence of a vertically twisted magnetization at the film surface and the Fe/W interface. A similar spin configuration may be induced by the external magnetic field and in the exchange-spring system;[15] here, it spontaneously occurs as a result of competing anisotropies.

The exact distribution of the magnetization directions was modeled by dividing the film with nominal thickness D (a fixed parameter of the fit for the given thickness) into N equithick sublayers, with $d = D/N$. For each sublayer, an in-plane orientation of the hyperfine magnetic field with a fixed value of 31 T ± 0.1 T (sublayer magnetization, M_N)

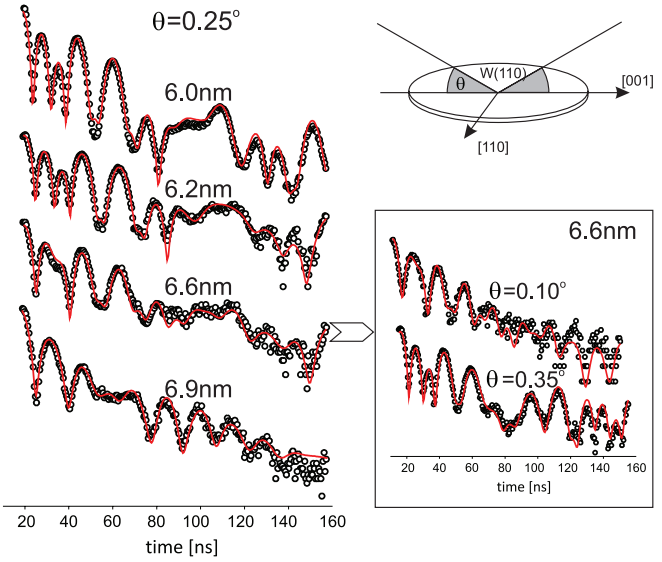

FIG. 2. (Color online) The NRS time spectra measured for the grazing incidence angle of $\theta = 0.25^\circ$ during the thickness-induced SRT at 250 °C are shown for the selected Fe thicknesses d (given in nm). The red line represents the fits obtained using the model with 16 sublayers. The inset shows the fitted time spectra recorded during the thickness-driven SRT process ($d = 6.6$ nm) for the grazing incidence angles of $\theta = 0.1^\circ$ and $\theta = 0.35^\circ$.

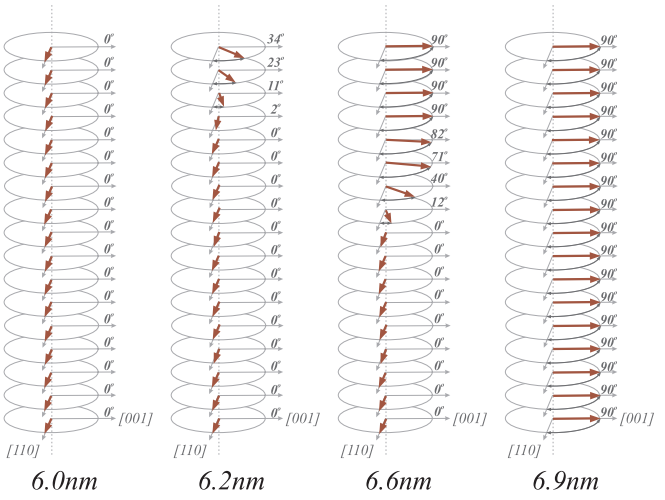

FIG. 3. (Color online) The evolution of the spin structure during the thickness-driven SRT at 250 °C derived from the NRS data is shown schematically as a function of the Fe thickness (indicated at the bottom in nm). The arrows represent the sublayer magnetizations. The angles φ_N between the magnetization vector and the $[1\bar{1}0]$ direction are given in degrees.

was defined by the angle φ_N with respect to the $[1\bar{1}0]$ in-plane direction. Accordingly, the only free parameters of the fits for increasing film thicknesses were the φ_N values. We examined the dependence of the quality of the fits on the number of sublayers N and observed that satisfactory fits could be obtained for 16 sublayers ($N = 16$), whereas higher numbers of the sublayers did not significantly improve the agreement between the fits and the measured spectra. For each nominal thickness, the fits of the spectra shown in Figs 2 and 3 were consistently obtained; therefore, the fitted magnetic structure was identical for all three GI angles. Note that a model assuming a smaller number of sublayers that have nonidentical thicknesses also successfully reproduced the measured time spectra and led to identical spectrum-dependent spin structures. This result indicates that the number of sublayers and also the sublayer thickness are important fit parameters that must be comparable with the length scale of the vertical magnetization direction distribution. The derived scenario of the thickness-induced SRT process at 250 °C is shown in Fig. 3. It is evident that, with increasing thickness, the reorientation of the magnetization to the [001] direction proceeds in such a way that the process is initiated at the top part of the Fe film and then a fanlike magnetization structure gradually develops with its center propagating towards the tungsten substrate as the Fe film grows. The spin fanning extends over a distance that corresponds to the thickness of five sublayers (∼2.5 nm) at the discussed intermediate state of the SRT process. Compared to the RT thickness-driven SRT,[9] at 250 °C, the sublayer switching is clearly opposite. Therefore, the conclusions concerning the role of specific magnetic anisotropy contributions to the SRT mechanism must be different. The magnetic surface anisotropy does not pin the magnetization direction to the $[1\bar{1}0]$ direction as strongly as it does at RT. It is caused by a different surface morphology that is characteristic for the films deposited at elevated temperatures and the temperature-induced weakening of the surface anisotropy. In fact, it can be concluded that magnetic surface anisotropy, although supporting the $[1\bar{1}0]$ orientation, cannot overcome the magnetocrystalline in-plane anisotropy of the top part of the Fe film and the effective magnetic anisotropy of the top part of the Fe film favors the [001] magnetization direction near the critical thickness. Within this picture, the magnetoelastic anisotropy originating at the Fe/W interface forces the magnetization orientation along $[1\bar{1}0]$ at lower thickness. The increase of the film thickness leads to the separation of the spin reorientation process for the top and bottom parts of the film via magnetic decoupling that results from the locally weakened exchange interaction. Then, similar to the RT thickness-induced SRT, the magnetoelastic anisotropy induces the change of the easy magnetization direction from $[1\bar{1}0]$ to [001] at a certain thickness and the SRT process is completed. A direct comparison of the thickness-driven SRTs at RT and 250 °C is difficult because the morphology of the Fe layers is very different for these two temperatures[20] and the elastic strains that are responsible for the magnetoelastic anisotropy effects are also most likely different. Nevertheless, the common feature of the thickness-induced SRTs is the evolution of the magnetoelastic anisotropy with the film thickness, which leads to the reorientation of its easy magnetization direction from $[1\bar{1}0]$ at a lower thickness to [001] above the critical SRT thickness. The weakening of the magnetoelastic anisotropy can lead to the magnetization reorientation from the $[1\bar{1}0]$ to the [001] direction because the latter is preferred by the magnetocrystalline anisotropy at all Fe thicknesses.

The final state of the thickness-driven SRT described above was the Fe film with a thickness of $D = 6.9$ nm magnetized along the [001] direction at 250 °C. For this sample, we observed the temperature-induced SRT process via the NRS

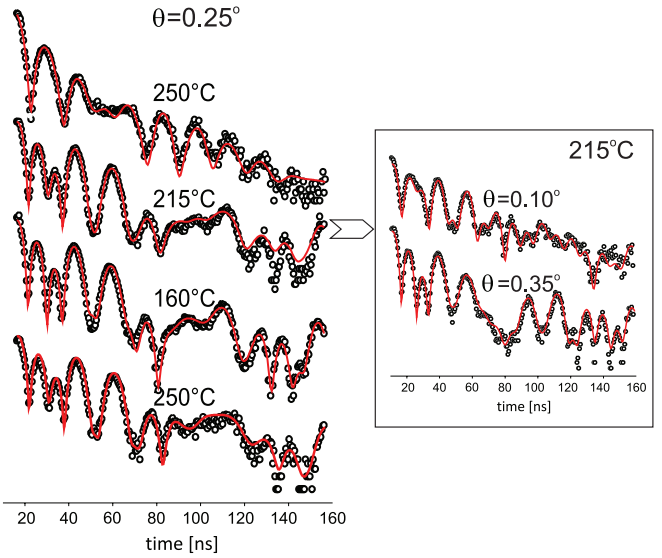

FIG. 4. (Color online) Fitted NRS time spectra collected for the 6.9-nm-thick Fe film during the following temperature cycle: 250 °C → 160 °C → 250 °C, from top to bottom, are shown for the grazing incidence angle of $\theta = 0.25°$.

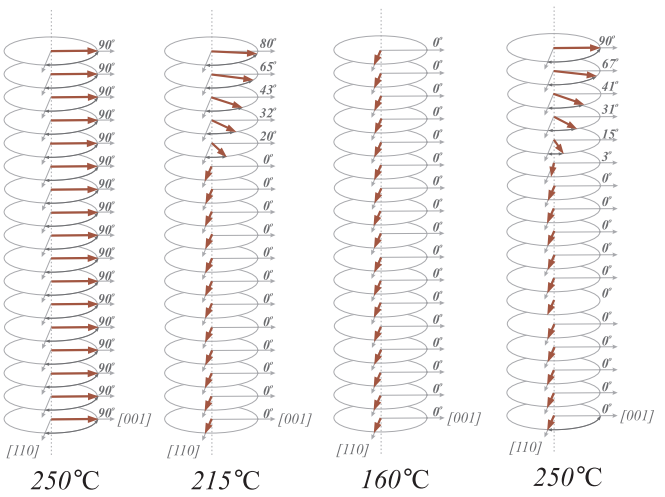

FIG. 5. (Color online) The evolution of the magnetic structure derived from the numerical analysis of the NRS time spectra collected during the temperature cycle of 250 °C → 160 °C → 250 °C for the 6.9-nm-thick Fe film on W(110). The arrows represent the sublayer magnetizations. The angles φ_N between the magnetization vector and the $[1\bar{1}0]$ direction are given in degrees.

measurements during cooling of the sample to RT. Note that the temperature-induced spin reorientation process makes experimental studies challenging because the increase of temperature may induce structural modifications, and in such a case, the separation of the temperature-driven evolution of the intrinsic magnetic (electronic) properties from the thermally induced structural changes is problematic. While the variation of the structural and electronic properties with temperature leads to the reversible SRT process, the morphological changes are often responsible for the irreversibility of the magnetization switching.[5] In addition, the adsorption of UHV residual gases can be responsible for the irreversibility of the SRT process, especially when the temperature of the system during spin reorientation is too low.

In our case, the growth of the film at 250 °C provided the required morphological stability for the temperature range between RT and 250 °C, which allowed for the pure temperature-driven SRT studies. The NRS time spectra measured for the 6.9-nm film at the GI angle of $\theta = 0.25°$ during the temperature cycle from 250 °C down to 160 °C and back to 250 °C are shown in the left panel of Fig. 4. The spectrum at 250 °C [Fig. 4(a)] reveals, according to the theoretical fit, a homogenous magnetization along the [001] direction (parallel to $\vec{k}_0$). After cooling the sample to 160 °C, the time spectrum [Fig. 4(c)] unambiguously indicated the magnetization switching to the $[1\bar{1}0]$ direction, which was confirmed by the consistent fit that assumed a homogenous magnetization perpendicular to $\vec{k}_0$. Further cooling to RT did not induce any modifications of this homogenous magnetization state, except for a further slight increase of B_{hf}. Deeper insight into the observed SRT process comes from the analysis of the time spectra measured at cooling for three GI angles at an intermediate temperature of 215 °C. The time spectrum measured at 215 °C for the low GI angle of $\theta = 0.1°$ has a very simple beat structure (see inset in Fig. 4), which is characteristic for the parallel alignment of the magnetization and $\vec{k}_0$ and indicates that the top layer (∼3 nm thick) of the Fe film is still magnetized along the [001] direction at this temperature. The orientation of the bottom part of the Fe film could be extracted from the shape of the time spectrum measured for the high GI angle of $\theta = 0.35°$, which clearly indicated the $[1\bar{1}0]$ magnetization orientation of the bottom part of the film at 215 °C. This straightforward observation of the noncollinear magnetization orientation of the top and bottom parts of the Fe film, with its surface magnetic moments parallel to the [001] direction and the Fe/W interface magnetized along the $[1\bar{1}0]$ direction, is confirmed by the numerical fits of the time spectra. The consistent fits for the three GI angles, which were performed using the same layered model as for the thickness-driven experiment discussed above, resulted in the magnetization structure shown in Fig. 5. The spin structure evolves between the homogenous [001] state at 250 °C and the $[1\bar{1}0]$ state at 160 °C via the vertically noncollinear magnetization distribution with the surface spins parallel to the [001] direction and the bottom part of the film magnetized along the $[1\bar{1}0]$ direction. The vertical width of the fan structure can be roughly estimated from the number of sublayers involved and is ∼2.5 nm, which is similar to the fanning at the thickness-induced transition discussed above. The observed SRT process proceeds with the change in temperature in an opposite manner than reported by Baberschke *et al.*[25] Ferromagnetic resonance measurements revealed that the magnetization reorients from the [001] direction at RT to the $[1\bar{1}0]$ direction at 330 °C for a 20-nm-thick Fe film deposited at 330 °C. This result was interpreted as arising from the different temperature dependencies of the magnetocrystalline anisotropy and the uniaxial in-plane magnetic anisotropy. Furthermore, the temperature dependence of the effective anisotropy constant K_{eff} reported in Ref. 25 for the films of different thicknesses clearly exhibit positive or negative slopes, which suggests that the reorientation transition is different depending on the film thickness. The simplest explanation for

the contradiction between our results and the ferromagnetic resonance data[25] can be associated with the differences in the Fe film structure related to the different growth process. Additionally, the adsorption of residual gases can also play a role. The residual gas adsorption, which is promoted at lower temperature, always decreases the critical SRT thickness leading to the stabilization of the [001] magnetization orientation.[26] For the NRS measurements, the complete set of the time spectra was collected in a few minutes and the residual gas adsorption effects are consequently minimized, especially at elevated temperatures, such as in the range between 250 °C and 160 °C.

Finally, the reversibility of the temperature-induced SRT process could be investigated by subsequently increasing the temperature from 160 °C to 250 °C. The corresponding time spectrum (Fig. 4) collected at 250 °C is very similar to the time spectrum measured at 215 °C during the cooling of the sample. Accordingly, the magnetic structure derived from the numerical analysis indicates the irreversibility of the temperature-induced SRT process, as shown in Fig. 5. We interpret the observed thermal hysteresis of the SRT process as arising from the unavoidable adsorption of UHV residual gases when cooling to 160 °C and subsequently to RT. The adsorbate is thermally desorbed during heating back to 250 °C. Because the SRT process is very sensitive to the adsorption of residual gases,[26] the desorption process during the temperature increase "slows down" the intrinsic temperature-induced spin reorientation to the [001] direction because the magnetic surface anisotropy supporting the $[1\bar{1}0]$ magnetization direction is simultaneously being gradually enhanced. The kinetics of the adsorption and desorption as a function of temperature are different, which results in the irreversibility of the SRT. Despite the complexity of the SRT mechanisms, an exotic noncollinear spin structure at the SRT process appears to be its general feature. Explaining this feature using the bulk-Fe material parameters, such as the exchange stiffness A and the magnetocrystalline anisotropy constant K, is not possible.[27] The observed magnetization fanning results in the increase of the free energy density ΔE_{ex} related to the exchange interaction that prefers a ferromagnetic spin alignment. ΔE_{ex} corresponding to the orthogonal sublayer magnetization orientation realized over the distance comparable to ∼3 nm (vertical fanning depth) can be roughly estimated as $A/3$ nm. Assuming the bulk value of $A \sim 2.8 \times 10^6$ erg/cm, one ends up with the $\Delta E_{ex} \sim 10$ erg/cm^2. ΔE_{ex} must be compensated by a decrease of the magnetic anisotropy energy of the bottom part of the film dominated by the magnetoelastic contribution. This result indicates a large change of the magnetoelastic anisotropy energy (per unit area) contribution that is involved in the SRT process. However, even the highest reported uniaxial magnetoelastic anisotropy energy $K_u \sim 0.8 \times 10^6$ erg/cm^3 (Ref. 11) yields for the Fe(110) film with a thickness of $D = 6$ nm the surface energy density of $K_u d \sim 0.5$ erg/cm^2 that can be attributed to the magnetoelastic effects, which is considerably less than the estimated ΔE_{ex}. This result suggests that not only enhanced anisotropies but also a softening of the exchange interaction must be present in the discussed Fe films, which are related to the (i) increased temperature, (ii) lattice expansion,[28] or (iii) dislocation-induced stacking faults. The above interpretation of the SRT process is in line with the experimental observation that the exchange stiffness parameter near the surface and Fe/W interface is reduced for a 4-nm-thick Fe film by a factor of 2.4 with respect to the bulk.[29]

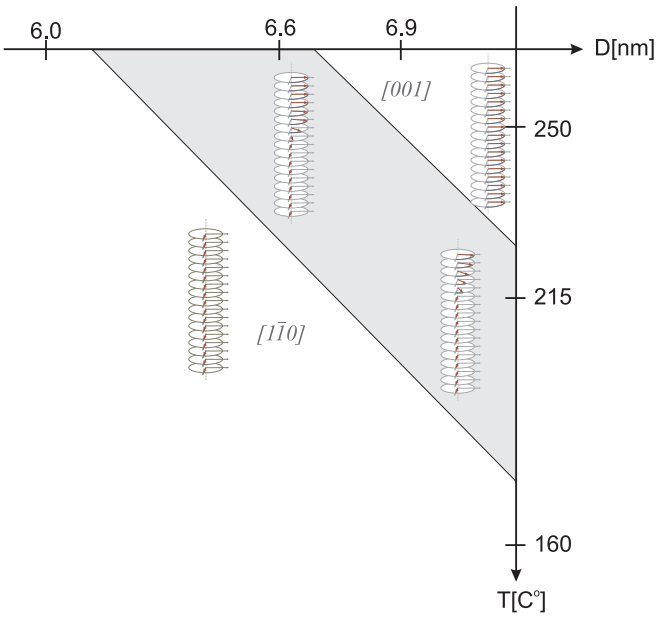

FIG. 6. (Color online) The thickness vs temperature phase diagram of the SRT process in the Fe(110) films grown at 250 °C derived from the thickness and temperature-dependent NRS studies.

The results concerning both of the SRT processes discussed above, namely, the thickness-driven reorientation at 250 °C and the temperature-driven transition, can be used to construct a schematic thickness-temperature phase diagram of the SRT process, which is shown in Fig. 6. The areas with the homogenous magnetization parallel to the $[1\bar{1}0]$ and [001] directions are separated by the shaded area of the intermediate noncollinear magnetization state. The slope of the solid line that separates this intermediate SRT state from the [001] magnetized state is uncertain because the SRT was only investigated as a function of temperature for one selected film thickness. It is provisionally assumed that the lines separating the intermediate state from the [001] and $[1\bar{1}0]$ magnetized states are parallel. This assumption can be justified by the similar temperature-driven evolution of the SRT process that is expected for the narrow Fe thickness range between 62 and 69 Å. The applicability of this phase diagram is limited to the Fe films deposited at 250 °C and investigated below this temperature. Especially at low thicknesses, the high transition temperature for the magnetization reorientation from the $[1\bar{1}0]$ to the [001] direction would certainly induce structural changes or even break a continuous film into islands.[30] Note that the observed thermal hysteresis effect has not been included in the phase diagram because it concerns the Fe films with adsorption-modified properties. Finally, note that the reported NRS analysis does not exclude the existence of multidomain transient states, which were recently observed in the SRT transition for Fe(110)/W(110) using x-ray magnetic circular dichroism-photoemission electron microscopy.[24] The appearance of the magnetic domains

that precede or follow the reported noncollinear magnetization states may be too rapid to be resolved in the NRS experiment.

IV. CONCLUSIONS

In conclusion, scenarios for the thickness-driven process at 250 °C and temperature-induced SRT processes were investigated for the Fe/W(110) system using the *in situ* nuclear resonant scattering of x rays. The most intriguing general feature of both transitions is a vertical noncollinear magnetic state that occurs during the reorientation between the $[1\bar{1}0]$ and [001] in-plane directions. In combination with the data concerning the RT thickness-induced transition,[9] the continuous and magnetically noncollinear nature appears to be a general feature of the SRT in the Fe/W(110) system. By varying the growth temperature, one can observe different noncollinear magnetization structures during the thickness-driven SRT process. It was shown that during the thickness-induced SRT process at 250 °C with increasing thickness, the magnetization reorientation from the $[1\bar{1}0]$ to the [001] direction is initiated by the topmost atomic layers and completed at the Fe/W(110) interface, whereas for the RT thickness-driven SRT, the sequence of the sublayer switching is opposite. However, the comparison of the thickness-driven SRT at 250 °C and the temperature-induced SRT indicates that the decrease of the temperature results in the scenario of the hypothetical inverse thickness-driven process.

ACKNOWLEDGMENTS

This work was supported in part by the Polish Ministry of Science and Higher Education and in part by the European Community under the project NMP4-CT-2003-001516 (DYNASYNC), as well as by the Team Program of the Foundation for Polish Science cofinanced by the European Regional Development Fund.

*Corresponding author: slezak@agh.edu.pl

†Present address: National Synchrotron Radiation Centre SOLARIS, Jagiellonian University, ul. Gronostajowa 7/P.1.6, 30-387 Kraków, Poland.

[1] U. Gradmann and J. Müller, Phys. Status Solidi **27**, 313 (1968).

[2] R. Allenspach, M. Stampanoni, and A. Bischof, Phys. Rev. Lett. **65**, 3344 (1990).

[3] R. Allenspach and A. Bischof, Phys. Rev. Lett. **69**, 3385 (1992).

[4] H. J. Elmers and U. Gradmann, Appl. Phys. A **51**, 255 (1990).

[5] P. J. Jensen and K. H. Bennemann, Surf. Sci. Rep. **61**, 129 (2006).

[6] H. P. Oepen, M. Speckmann, Y. Millev, and J. Kirschner, Phys. Rev. B **55**, 2752 (1997).

[7] A. Stupakiewicz, A. Maziewski, K. Matlak, N. Spiridis, M. Ślęzak, T. Ślęzak, M. Zając, and J. Korecki, Phys. Rev. Lett. **101**, 217202 (2008).

[8] D. Wilgocka-Ślęzak, K. Freindl, A. Kozioł, K. Matlak, M. Rams, N. Spiridis, M. Ślęzak, T. Ślęzak, M. Zając, and J. Korecki, Phys. Rev. B **81**, 064421 (2010).

[9] T. Ślęzak, M. Ślęzak, M. Zając, K. Freindl, A. Kozioł-Rachwał, K. Matlak, N. Spiridis, D. Wilgocka-Ślęzak, E. Partyka-Jankowska, M. Rennhofer, A. I. Chumakov, S. Stankov, R. Rüffer, and J. Korecki, Phys. Rev. Lett. **105**, 027206 (2010).

[10] U. Gradmann, J. Korecki, and G. Waller, Appl. Phys. A **39**, 101 (1986).

[11] D. Sander, A. Enders, and J. Kirschner, J. Magn. Magn. Mater. **200**, 439 (1999).

[12] S. Couet, Th. Diederich, S. Stankov, K. Schlage, T. Slezak, h R. Rüffer, J. Korecki, and R. Röhlsberger, Appl. Phys. Lett. **94**, 162501 (2009).

[13] D. Kmieć, B. Sepiol, M. Sladecek, M. Rennhofer, S. Stankov, G. Vogl, B. Laenens, J. Meersschaut, T. Ślęzak, and M. Zając, Phys Rev. B **75**, 054306 (2007).

[14] *Nuclear Resonant Scattering of Synchrotron Radiation*, edited by E. Gerdau and H. de Waard, Hyperfine Interact. Vol. 123–125 (Springer, New York, 1999).

[15] R. Röhlsberger, H. Thomas, K. Schlage, E. Burkel, O. Leupold, and R. Rüffer, Phys. Rev. Lett. **89**, 237201 (2002).

[16] R. Röhlsberger, J. Bansmann, V. Senz, K. L. Jonas, A. Bettac, K.-H. Meiwes-Broer, and O. Leupold, Phys. Rev. B **67**, 245412 (2003).

[17] W. Sturhahn, Hyperfine Interact. **87**, 149 (2000).

[18] R. Rüffer and A. I. Chumakov, Hyperfine Interact. **97-98**, 589 (1996).

[19] S. Stankov, R. Rüffer, M. Sladecek, M. Rennhofer, B. Sepiol, G. Vogl, N. Spiridis, T. Slęzak, and J. Korecki, Rev. Sci. Instrum. **79**, 045108 (2008).

[20] M. Albrecht, T. Furubayashi, M. Przybylski, J. Korecki, and U. Gradmann, J. Magn. Magn. Mater. **113**, 207 (1992).

[21] T. Ślęzak, J. Łażewski, S. Stankov, K. Parliński, R. Reitinger, M. Rennhofer, R. Rüffer, B. Sepioł, M. Ślęzak, N. Spiridis, M. Zając, A. I. Chumakov, and J. Korecki, Phys. Rev. Lett. **99**, 066103 (2007).

[22] J. Korecki and U. Gradmann, Phys. Rev. Lett. **55**, 2491(1985).

[23] M. Przybylski, U. Gradmann, and J. Korecki, J. Magn. Magn. Mater. **69**, 199 (1987).

[24] E. Vescovo, T. O. Mentes, J. T. Sadowski, J. M. Ablett, M. Á. Niño, and A. Locatelli, Phys. Rev. B **82**, 184405 (2010).

[25] F. Gerhardter, Y. Li, and K. Baberschke, Phys. Rev. B **47**, 11204 (1993).

[26] D. Yu, C. Math, M. Meier, M. Escher, G. Rangelov, and M. Donath, Surf. Sci. **601**, 5803 (2007).

[27] M. Rybicki and I. Zasada, J. Phys.: Condens. Matter **24**, 386005 (2012).

[28] S. Stankov, R. Röhlsberger, T. Ślęzak, M. Sladecek, B. Sepioł, G. Vogl, A. I. Chumakov, R. Rüffer, N. Spiridis, J. Łażewski, K. Parliński, and J. Korecki, Phys. Rev. Lett. **99**, 185501 (2007).

[29] J. Korecki, M. Przybylski, and U. Gradmann, J. Magn. Magn. Mater. **89**, 325 (1990).

[30] V. Senz, R. Röhlsberger, J. Bansmann, O. Leupold, and K.-H. Meiwes-Broer, New J. Phys. **5**, 47.1 (2003).